

VHDL Module for the R Wave Detection in Real Time Using Continuous Wavelet Transform

Frank Martínez-Suárez

Bioelectronics Section, Department of Electrical Engineering
CINVESTAV

Mexico City, Mexico
frank.martinez@cinvestav.mx

Carlos Alvarado-Serrano

Bioelectronics Section, Department of Electrical Engineering
CINVESTAV

Mexico City, Mexico
calvarad@cinvestav.mx

Abstract— In this work, we propose a module designed in VHDL for FPGA that detects the R wave and calculates the duration of the RR interval beat to beat in the electrocardiogram (ECG) to obtain the heart rate in real time using the continuous spline wavelet transform in 2 leads. The article describes the elements that make up the module and analyzes its performance with five 30 min and one 24 h ECG recordings. The VHDL module of R wave detector has an accuracy greater than 90%, with a 1.35% in aVF lead in 30 min records, and 2.13% error in DI lead and 9.9% error in aVF lead in 24 h recordings. Therefore, the analysis of the heart rate variability (HRV) in short and long ECG recordings with this module implemented in a FPGA can be done.

Keywords— FPGA, VHDL, ECG, R wave detector, Heart Rate, Wavelet Transform

I. INTRODUCTION

The electrocardiography is a useful tool for diagnosis and treatment of many cardiovascular diseases, which are among the main causes of mortality worldwide [1]. Measurements of electrocardiogram (ECG) time intervals like RR interval or heart rate changes are important for the analysis of the heart rate variability (HRV), which is used to investigate cardiological and non-cardiological diseases, to assess autonomic nervous responses and risk of cardiovascular death or arrhythmic events [2,3]. For the HRV measurement, QRS complex detection is necessary to obtain the heart rate. Many algorithms have been proposed for QRS detection, some approaches are based on: signal derivatives and digital filters, wavelet transform (WT), filter bank, neural networks, adaptive filters, hidden Markov models, mathematical morphology, matched filters, genetic algorithms, Hilbert transform, length and energy transforms and syntactic methods [4].

With the advancement of Field Programmable Gate Array (FPGA) technology various algorithms have been implemented for the real-time QRS complex detection to determine the heart rate [5–8]. A useful tool to detect ECG waves as QRS complex is the WT, because of its ability to detect transients and its robustness in front of noise and artifacts. WT at different scales describe the time characteristics of a signal in different frequency bands; therefore it is adequate to analyze the ECG, which it has waves with different frequency content like noise and artifacts affecting the ECG that can be reduced [9–11].

In this work, we propose the design of a VHDL module that detects the R wave and calculates the duration of the RR interval beat to beat to obtain the heart rate in real time using the continuous wavelet transform (CWT) with splines.

II. MATERIALS AND METHODS

The implementation of the VHDL module for the detection of the R wave and the obtaining of the heart rate in real time using the CWT was developed with the software Vivado 2017.4 and was tested in the development card Basys 3 of Xilinx [12], that has an FPGA XC7A35T-ICP236C which belongs to the Artix-7 family.

A. Continuous Wavelet Transform

The CWT is defined in equation 1 [13]:

$$CWTx(a, b) = \frac{1}{\sqrt{a}} \int_{-\infty}^{\infty} X(t) \psi^* \left(\frac{t-b}{a} \right) dt \quad (1)$$

Where the parameter b indicates a translation, the parameter a indicates a scaling, the function $X(t)$ is the signal and $\psi^*(t)$ is the conjugate complex of the mother wavelet function $\psi(t)$.

Depending on the mother wavelet function $\psi(t)$ different results will be obtained on the parameters that we want to analyze from the signal $X(t)$, but the function $\psi(t)$ must comply with finite energy (2), which has a transform of Fourier (3) and a band pass filter behavior (4).

$$E = \int_{-\infty}^{\infty} |\psi(t)|^2 dt \quad (2)$$

$$\widehat{\psi}(\omega) = \int_{-\infty}^{\infty} \psi(t) e^{-i\omega t} dt \quad (3)$$

$$C_g = \int_{-\infty}^{\infty} \frac{|\widehat{\psi}(\omega)|^2}{\omega} dt \quad (4)$$

Where ω is called the angular frequency and C_g the admissibility condition

B. Determination of the scale in the CWT

The first step for the determination of the heart rate consisted in the determination of the scale of the CWT to be used.

This work has been funded by a scholarship from the CONACYT (Mexico) to Frank Martínez-Suárez.

For this, as shown in Table I, a comparison of the cutoff frequencies was made: low (fc1) and high (fc2), of the different scales of the CWT, from 1 to 12, with a sampling frequency of 1000 Hz.

TABLE I. CUTOFF FREQUENCIES OF THE FILTER PASS BAND CREATED BY THE CWT

Escala	Fc1 (Hz)	Fc2 (Hz)
1	112	373
2	58	192
3	39	129
4	29	97
5	23	78
6	19	65
7	17	55
8	14	49
9	13	43
10	12	39
11	11	35
12	10	32

In the module we select the scale 8 for a sampling frequency of 1000 Hz, the main reason for the selection of this scale is that its bandwidth is between 14 Hz and 49 Hz, which allows us to minimize the interference caused by the 60 Hz frequency generated by the power line and better fits the QRS complex bandwidth of the ECG signal, 10 Hz at 30 Hz [14] (Fig. 1).

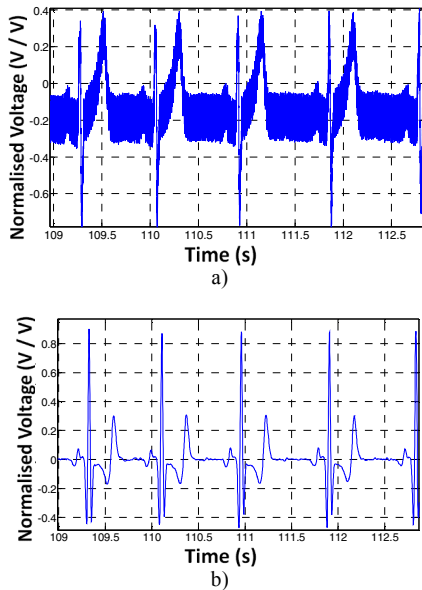


Fig. 1. DI lead ECG (a) and its CWT at scale 8 (b).

Once the scale was defined, we proceeded to design the module for obtaining the heart rate, in which two functions were defined: the CWT implementation and the R wave detection. For the correct functioning of these two functions, four modules were created:

- First module to obtain the CWT.
- Second module for obtaining the CWT.
- Third module for obtaining the CWT.
- Module for the R wave detection.

The first requirement of the module for obtaining the heart rate is that it must be able to process the signal as the samples are digitized, so that if it receives a value, it delivers a value. For this purpose, each module stores the previous results that it needs to calculate the next value to deliver. The operation of the module for obtaining the heart rate is based on the principle of the state machine of Fig. 2.

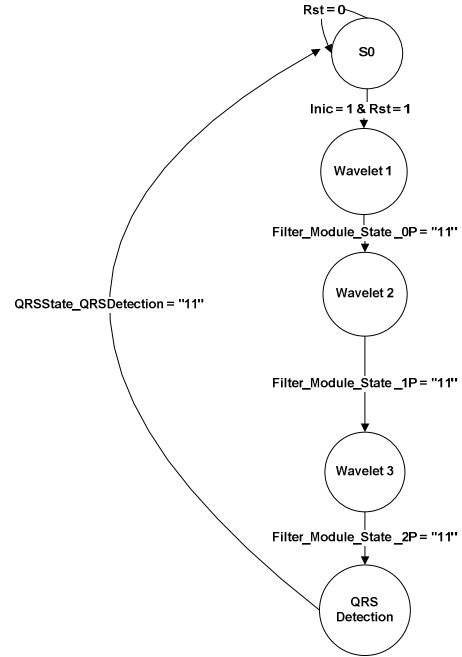


Fig. 2. State machine for obtaining the heart rate (Note: When the signal Rst = 0 the next state is always S0, it was not included for better understanding the diagram).

The state machine of Fig. 2 starts its operation when the input signals "Inic" and "Rst" are equal to one, which indicates that a new sample exists for analysis. When this condition is met, the first module to obtain the CWT processes the received sample and delivers it to the second module to obtain the CWT, which processes the result obtained from the previous module and delivers it to the third module for obtaining the CWT, the result delivered by the third module of the CWT is used by the module for the R wave detection to calculate the heart rate in lat/m. The module for the R wave detection updates its output value each time that the detection of a new R wave is completed.

C. Modules for obtaining the CWT with splines

To obtain the CWT with splines, the implemented algorithm was based on the proposal made by Unser et al. [13]. In particular, the first derivative of order two of the cubic spline was the wavelet function $\psi(t)$ used in this work. For the development of the algorithm, most of the steps described in the mentioned article were followed, but small modifications were developed to facilitate its implementation in the FPGA.

In the first module to obtain the CWT with splines, a prefilter is made to the input signal as a result of the convolution of the B-spline coefficients and the input signal, (5) [13];

$$s_1(k) := \langle s(x), \beta^{n_2}(x-k) \rangle = b^{n_1+n_2+1} * (b^{n_1})^{-1} * s[k] \cong b^{n_2} * s[k] \quad (5)$$

The filter $b^{n_1+n_2+1}$ is a symmetric kernel of finite impulse response (FIR), which is characterized by a vector b of size $n_b = n_1 + n_2 + 1$ that contains the filter coefficients. Where $n_1 = 1$, which indicates that the signal is linear between samples and $n_2 = 3$, which indicates that the spline degree is cubic.

The coefficients of vector b obtained present the problem of being rational numbers between "1" and "0" which makes the filter implementation in the FPGA difficult, to correct this problem we multiply the coefficients by 2^{16} and rounding off the result to integer numbers (table II). This process does not significantly affect the operation of the filter with respect to the frequency components, but it affects the amplitude of the resulting signal, so that it is necessary to divide it by 2^{16} to compensate for the multiplication made to the coefficients.

TABLE II. UNMODIFIED AND MODIFIED COEFFICIENTS OF THE FILTER IMPLEMENTED.

Unmodified coefficients	Coefficients multiplied by 2^{16}
0.0083	543
0.2167	14201
0.5500	36044
0.2167	14201
0.0083	543

In the second module to obtain the CWT, a moving sum filter was implemented, defined in (6) [13]:

$$s_m(k) := \langle s(x), \beta^{n_2}((x-k)/m) \rangle = u_m^{n_2} * s_1[k] \quad (6)$$

In the third module to obtain the CWT, a filtering is performed with the B-spline coefficients of the wavelet $\psi(t)$, defined in (7) [13]:

$$\omega_m(k) = [p]_{1m} * s_m[k] \quad (7)$$

The FIR operator p is characterized as a vector p of size n_p shown in [13].

D. Module for the R wave detection

The design of the module for the R wave detection was based on the algorithm developed by Alvarado et al. [11], which was modified to achieve the R wave detection and to calculate the duration of RR interval beat to beat to obtain the heart rate in real time. To detect the duration of the RR interval, it is sufficient to know the separation between the different zero crossings P1 of two consecutive QRS complexes which represent the R wave peak (Fig. 3).

As it is shown in Fig. 3, the complexity of the process is the detection of point P1; since this point has a value (zero) very common in the results of the CWT. To enable the detection of point P1, the state machine shown in Fig. 4 was implemented, which has five fundamental stages.

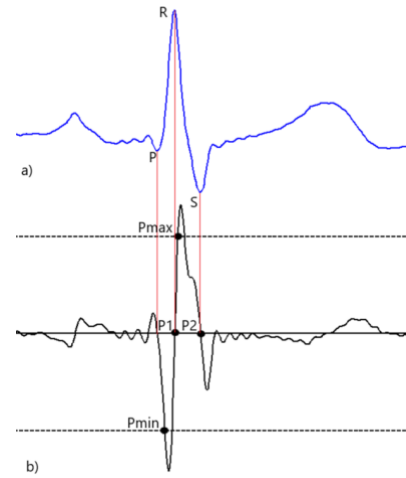


Fig. 3. ECG (a) and CWT at scale 3 (b).

The first stage is responsible for detecting the Pmin point by comparing the received value of the modules to obtain the CWT with the value stored in the variable "Output_Memory_Pmin".

The second stage is subdivided in three functions:

- The first function is to detect if the value received from the modules for obtaining the WT multiplied by 0.75 is less than that stored in the variable "Output_Memory_Pmin", if positive, the variable "Output_Memory_Pmin" is updated, assigning it the value received from the modules for obtaining the CWT multiplied by 0.75.
- The second function is the detection of point P1 when the value received from the modules for obtaining the CWT has a value of zero.
- The third function consists of copying the value of the time counter in the variable "OutputSignalQRS" (duration of the RR interval) when the P1 point is detected and restarting the counter.

The third stage is responsible for the detection of the Pmax point by comparing the received value of the modules for obtaining the CWT with the value stored in the variable "Output_Memory_Pmax".

The fourth stage is sub divided into two functions:

- The first function is to detect if the value received from the modules for obtaining the CWT multiplied by 0.75 is greater than that stored in the variable "Output_Memory_Pmax" if the variable "Output_Memory_Pmax" is updated, assigning it the value received from the modules for obtaining the CWT by 0.75.
- The second function focuses on the detection of point P2 when the value received from the modules for obtaining the CWT has zero value.

The fifth stage is responsible for performing a delay of 80 ms before starting the cycle again, to avoid possible confusion due to noise in the signal or the T wave.

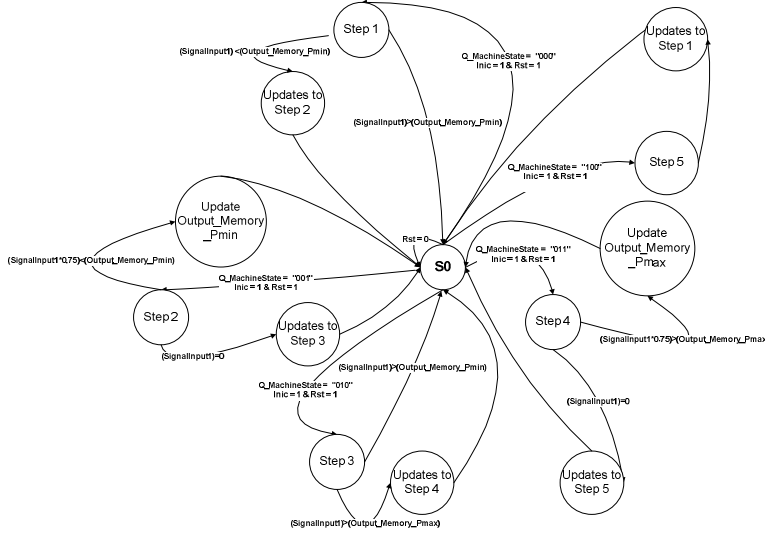


Fig. 4. State machine for the detection and calculation of the RR interval duration. (Note: When the signal Rst = 0 the next state is always S0, it is not included for better understanding of the diagram).

III. RESULTS

A. Validation of the R wave peak detection algorithm

For the verification of the module, it was used in a prototype of ambulatory monitor and three tests were carried out. In the first test, the device was stimulated with an ideal synthetic signal (without any type of noise) obtaining a detection of the R wave of 100%. In the second test, two 30 min recordings in DI and aVF leads were taken in 5 healthy subjects at rest. The third test was a 24 h recording in DI and aVF leads of a healthy male subject. From the records taken, the first minute was eliminated, which is the time the module uses to calibrate itself (assign the work values to "Output_Memory_Pmax" and "Output_Memory_Pmin").

B. Second test

Figure 5 shows an excerpt of the ECG recordings of the two leads and the result of the R wave detection of a subject.

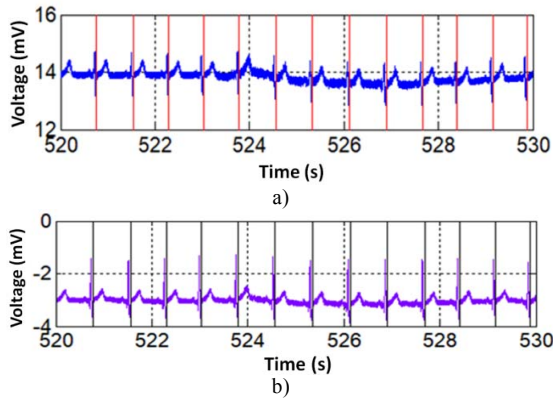


Fig. 5. ECG excerpts with R wave detection obtained from subject 4, DI lead (a), aVF lead (b).

Table III shows the results obtained in the R wave detection, performed in the aVF lead in the 5 subjects. From this table, 10694 beats were analyzed with 62 false detections for an accuracy of 99.4% (error=0.58%).

TABLE III. EVALUATION OF THE ALGORITHM OF R WAVE DETECTION IN THE aVF LEAD.

Subject	Beats	False Positive	False Negative	False Detections
1	2136	0	11	11
2	2001	0	1	1
3	2050	0	20	20
4	2292	0	0	0
5	2215	0	30	30
Total	10694	0	62	62

For the analysis of the RR interval variability, the results of the aVF lead were used. Table IV shows that subject 3 has the greatest RR variability, and the subject 5 has the lowest RR variability.

TABLE IV. STATISTICAL ANALYSIS OF THE RR INTERVAL VARIABILITY IN THE 30 MIN RECORDS

Subject	Mean value of the RR interval	Standard deviation of RR interval
1	0.8695	0.1107
2	0.7854	0.0833
3	0.8189	0.1170
4	0.7589	0.0704
5	0.8093	0.0593

C. Third test

The performance of the R wave detection algorithm in the 24 h recordings is shown in Table V with the results of the DI and aVF leads. As can be seen in the table, there are the total error percentages of each lead, incurring an error of 9.93% for the aVF lead and 2.13% for the DI lead, presenting the main

failures due to the presence of noise and artifacts in the signal acquisition.

TABLE V. R WAVE DETECTION FOR THE HEART RATE CALCULATION IN DI AND AVF LEADS

Lead	Beats	False Positive	False Negative	% False Detections	Mean Heart Rate lat / min
DI	105750	2083	169	2.13	73.44
aVF	105750	10306	192	9.93	73.44

IV. CONCLUSIONS

In this work, the preliminary results of the design and implementation of a VHDL module for the R wave detection based in the CWT with splines and the obtaining of the heart rate in real time were shown. The data obtained by the module will allow the patient to monitor and detect heart rate abnormalities with a delay of less than 20 ms. As well as the possibility that the results are stored in a micro SD memory so that they can be examined by a cardiologist for the detection of diseases or for their processing with programs for the location of anomalies in the ECG. Despite the fact that the module showed perfect results in the R wave detection with synthetic signals, when it was used in a system with real patient signals, its efficiency was reduced due to the noise and artifacts introduced by the electrodes, but it maintained a percentage of accuracy over 90%.

Therefore, although the designed module can be improved, its implementation in electrocardiographic devices of long and short duration implemented in an FPGA is possible, and the analysis of the HRV can be done. For the function test of the module in VHDL, no special characteristics were analyzed in the test subjects, but for a better validation of the device in the future its performance will be analyzed with recordings from the MIT-BIH arrhythmia database.

REFERENCES

- [1] World Health Organization (WHO). (24/5/2018). "The top 10 causes of death," In: News, Fact sheets, Detail, Available from: <https://www.who.int/news-room/fact-sheets/detail/the-top-10-causes-of-death> [Accessed: 19/3/ 2019]
- [2] Task Force of The European Society of Cardiology and The North American Society of Pacing and Electrophysiology, "Heart rate variability standards of measurement, physiological interpretation and clinical use," *Eur. Heart J.*, vol. 17, pp. 354–381, 1996.
- [3] R.E. Kleiger, P.K. Stein, J.T. Bigger Jr., "Heart rate variability: measurement and clinical utility," *Ann. Noninvasive Electrocardiol.*, vol. 10, no. 1, pp. 88–101, 2005.
- [4] B.-U. Köhler, C. Hennig, R. Orglmeister, "The principles of software QRS detection," *IEEE Eng. Med. Biol. Mag.*, vol. 21, issue 1, pp. 42–57, 2002.
- [5] A. Shukla and L. Macchiarulo, "A fast and accurate FPGA based QRS detection system," in *Proc. 2008 30th Annual International Conference of the IEEE Engineering in Medicine and Biology Society (EMBS)*, Vancouver, BC, Canada, pp. 4828–4831.
- [6] R. Stojanović, D. Karadaglić, M. Mirković, D. Milošević, "A FPGA system for QRS complex detection based on integer wavelet transform," *Measurement Science Review*, vol. 11, no. 4, pp. 131–138, 2011.
- [7] H.K. Chatterjee, R. Gupta, J.N. Bera, M. Mitra, "An FPGA implementation of real-time QRS detection," in *Proc. 2011 2nd International Conference on Computer and Communication Technology (ICCT-2011)*, Allahabad, India, pp. 274–279.
- [8] T. Li, Yi. Ma, Yu. Ma, X. Lu, "The real-time R-wave detection based on FPGA," in *Proc. 2014 7th International Conference on BioMedical Engineering and Informatics (BMEI 2014)*, Dalian, China, pp. 393–398.
- [9] C. Li, C. Zheng, C. Tai, "Detection of ECG characteristic points using wavelet transforms," *IEEE Trans. Biomed. Eng.*, vol. 42, no. 1, pp. 21–28, 1995.
- [10] J. P. Martínez, R. Almeida, S. Olmos, A. P. Rocha, P. Laguna, "A wavelet-based ECG delineator: evaluation on standard databases," *IEEE Trans. Biomed. Eng.*, vol. 51, no. 4, pp. 570–581, 2004.
- [11] C. Alvarado, J. Arregui, J. Ramos, R. Pallás-Areny, "Automatic detection of ECG ventricular activity waves using continuous spline wavelet transform," in *Proc. 2005 2nd. International Conference on Electrical and Electronics Engineering (ICEEE)*, Mexico City, Mexico, pp. 189–192
- [12] Basys3 TM FPGA Board Reference Manual, Digilent Inc., 2014.
- [13] M. Unser, A. Aldroubi, S.J. Schiff, "Fast implementation of the continuous wavelet transform with integer scales," *IEEE Trans. Signal Process.*, vol. 42, no. 12, pp. 3519–3523, 1994.
- [14] W. J. Tompkins, *Biomedical Digital Signal Processing*, 1st ed. Saddle River, New Jersey: Prentice Hall, 2000.